

DEUTSCHES ELEKTRONEN-SYNCHROTRON
in der HELMHOLTZ-GEMEINSCHAFT
DESY SUMMER STUDENT PROGRAM 2008



First Data Quality of the CALICE Test Beam
2008

by

Susanne Jungmann

University of Heidelberg

23.07. - 16.09.2008

Supervisor: Dr. Erika Garutti

NOTKESTRASSE 85 - 22607 HAMBURG

Abstract

This work is the result from an eight-week summer student program at the *Deutschen Elektronen-Synchrotron DESY* during the summer 2008. In here the first online data quality results from the 2008 test beam at the *Fermi National Accelerator Laboratory (FNAL)* shall presented. This includes studying the performance of the analogue hadronic calorimeter during the latest FNAL test period, which means its quality while operating at different beam energies as well as stability studies concerning the provided beam.

Zusammenfassung

Diese Arbeit ist Resultat eines acht wöchigen Sommer Studenten Programms am *Deutschen Elektronen-Synchrotron DESY* im Sommer 2008. Es sollen hier die ersten Ergebnisse der online Datenanalyse des Teststrahls 2008 am *Fermi National Accelerator Laboratory (FNAL)* vorgestellt werden. Dies beinhaltet das Analysieren der Performance des analogen Hadronenkalorimeters während der letzten Testphase am FNAL, was die Überprüfung der Qualität des Kalorimeters bei verschiedenen Strahlenergien ebenso wie Stabilitätsuntersuchungen des bereitgestellten Strahls bedeutet.

1 Introduction - The CALICE AHCAL Physics Prototype

Already years ago one started to think about the next particle physics project following the proton-proton collider LHC at the *Conseil Européen pour la Recherche Nucléaire (CERN)*. Due to this fact the next generation of particle colliders will be the International Linear Collider (ILC) for electrons and positrons able to deliver center of mass energies up to 1 TeV. The hope is that this collider will be capable of giving even deeper insights into the discoveries from the LHC and thereby point the way to the future of particle physics. The high precision needed for these measurements requires an excellent detector. Since a typical event at the ILC will be a multi-jet event the calorimetry plays an important role to distinguish for example W and Z bosons. Therefore one needs at least an energy resolution better than $30\%/\sqrt{E}$ (see figure 1).

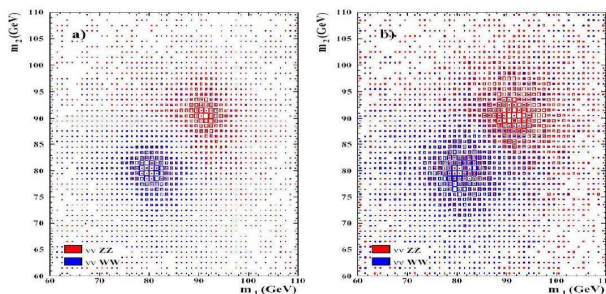


Figure 1: Energy resolution for W and Z bosons in multiple jet final states. Left as proposed for the ILC and right as achieved for the LEP experiments

This can be achieved with high granularity in longitudinal and transverse directions for both the electromagnetic (ECAL) and the hadronic (HCAL) calorimeter. Such a prototype for an analogue hadronic calorimeter (AHCAL) in combination with the so called particle-flow concept was built in 2006 within the collaboration for a *CAlorimeter for the LInear Collider Experiment* at the *Deutsches Elektronen-Synchrotron (DESY)* in Hamburg, Germany. The AHCAL subgroup has build a $1m^3$ sandwich calorimeter called physics prototype with 2 cm steel plates as absorber material and small scintillator tiles as active material. The high granularity is achieved by 38 scintillator tile layers ($90 \times 90 \text{ cm}^2$) along a depth of 4.5 interaction lengths. The first 30 layers are more sensitive and consist of 216, the last 8 layers consist due to cost reasons only of 141 single plastic scintillator tiles. The calorimeter consists of $3 \times 3 \text{ cm}^2$ tiles in the center (100 tiles), surrounded by a large area covered with $96 \text{ } 6 \times 6 \text{ cm}^2$ tiles and finally enclosed by an outer

ring of 20 $12 \times 12 \text{ cm}^2$ tiles (see figure 2). MC studies show that such a tile pattern allows excellent longitudinal and transverse reconstruction of the particle shower. The 7608 tiles in total are read out individually by new

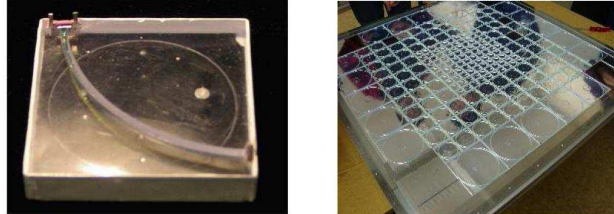


Figure 2: Tile mosaic of the physics prototype

semiconductor based photodetectors called silicon photomultiplier (SiPMs) that are insensitive to large magnetic fields. Inside is a wavelength-shifter fiber which illuminate a small photo-detector. Data taking with this prototype started in 2006 at CERN at the *Super Proton Synchrotron (SPS)* until 2007 and was continued in 2008 at the *Fermi National Accelerator Laboratory, Chicago, Illinois (FNAL)* by moving the detector system there to analyse the response of the detector to low energetic particles (see figure 3).



Figure 3: Detector system at FNAL

2 Physics in a Hadronic Calorimeter

One has in principal to differentiate between two types of hadronic calorimeters: homogeneous calorimeters consisting of blocks of sensitive absorber material and sampling calorimeters where the particle's energy is measured within active layers that are interleaved with passive absorber layers. The later class was used for the physics prototype discussed here (see figure 4).

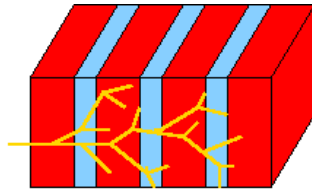


Figure 4: Hadronic sandwich calorimeter, absorber material (red) interleaved with scintillators (blue)

To achieve a good three dimensional picture of the shower cascade with time the amount of active material in front of the calorimeter has to be minimised. That's why besides other devices the hadronic calorimeter is placed inside of the magnetic coil for the ILC experiment.

In general a hadronic calorimeter is designed to measure particles that interact via the strong nuclear force. Most particles by entering the hadronic calorimeter initiate a particle shower while depositing all its energy in the calorimeter down to the threshold of ionisation and excitations that are detectable by the readout electronics. The basic mode of operation of a calorimeter is the proportionality of the deposited energy to the light produced in the active layers. It can be detected with photo detectors, that convert light into an electric signal. The higher the energy of the incoming particle, the more secondary particles it will produce, and therefore the bigger the measured signal will be. Since there is a variety of processes in a hadronic shower that may occur, hadronic showers are broad and deep and thus complicate to analyse. If a hadronic particle is not interacting inelastically with the absorber material it is only losing energy via ionisation and excitations of the absorber layers. The probability of such an inelastical interaction is given by

$$P_{inelastical} = 1 - e^{-x/\lambda_0},$$

where λ_0 is the *nuclear interaction lenght*. It describes the average distance a high energetic hadron travels through a medium before interacting strongly. Therefore the scales of the designed hadronic calorimeter have to be defined

by λ_0 . In figure 5 a sketch of such an hadronic shower is displayed. The path at the very beginning is as above mentioned defined by the nuclear interaction length. The cascade can be divided into three components: the hadronic part, the electromagnetic part and furthermore the neutron component.

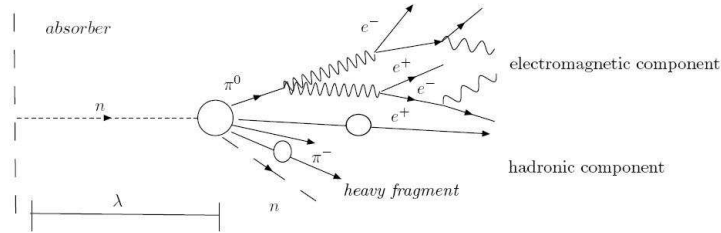


Figure 5: Schematic of a hadronic shower development

All these different processes were displayed already during data taking via the online monitoring histograms and shall be analysed in more detail in the following chapter.

3 Data Quality Analysis

The experimental setup at the FNAL for the test beam 2008 was the following:

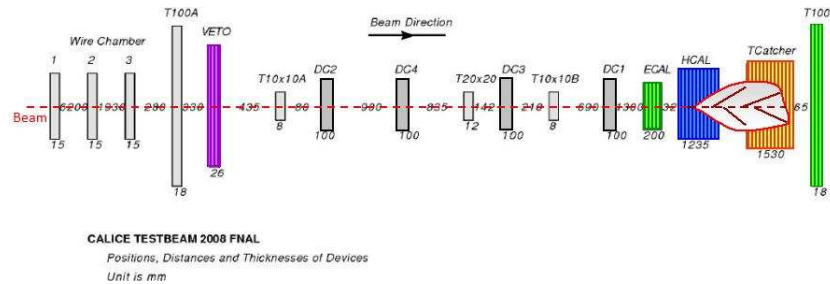


Figure 6: Experimental Setup at FNAL in 2008

One can see the four drift chambers followed by a silicon-tungsten ECAL and the AHCAL. The tail catcher and the muon trigger (TCMT) form the end of the detector and work in principal with the same technology than the AHCAL. At the beginning the Veto ADC Trigger is placed. Most of the time the ECAL stood in front of the AHCAL but was removed for some late runs in July out of the beamline. The energy of the beam varied between 1 GeV up to 120 GeV and contained electrons, positrons, pions, protons

and muons or a mixture of some of them. In total $\approx 60\text{ Mio.}$ events were collected in 2008 which is equal to 951 runs (see figure 7). But most of them were calibration or test runs besides for example electron or muon runs. The

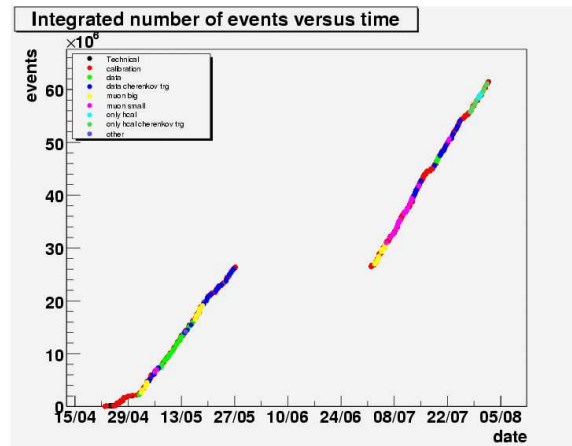


Figure 7: Total number of events taken in 2008 at FNAL

goal of my work was to analyse all 2008 physics runs and provide at the end a list including all the good and easy analysable runs for analysers and a list with all the problematic runs for the experts to analyse them more precisely. I applied three cuts to all runs. First runs with less than 10.000 detected events are not used since most of them were stopped too early or problems occurred. Second I am not able to analyse runs with an energy smaller or equal to 4 GeV because as one will see later my reconstruction methods don't work for these runs (see section 3.1). And finally I include only pion and proton runs. So out of all runs only 158, which is about 16%, are used for a first online analysis. The results of these measurements were plotted in several histograms to give already while running the experiment an impression of the overall quality. All applied settings were written down in an electronic logbook on the internet so everybody from the CALICE collaboration was able to look at the newest data. This is also useful for later studies of problems that might be explainable with the notations in the logbook. To begin with I did some statistics plots. Figure 8 shows the number of events taken for different energies and different incident angles of the AHCAL towards the beamline at all available energies. As one can see the main part of the runs was collected at an angle of 0° and energies around 20 or 30 GeV.

A nice example event is shown in figure 9. One can see the ECAL, AHCAL and the TCMT in this three dimensional demonstration as well as

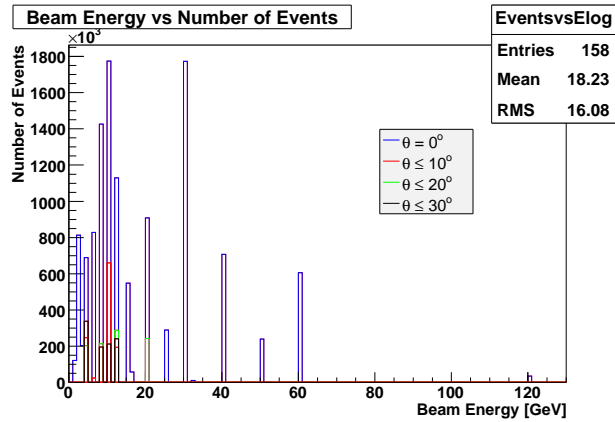


Figure 8: Overall statistics plot for all energies and all incident angles of the AHCAL

the hadronic shower starting in the AHCAL and developing further on.

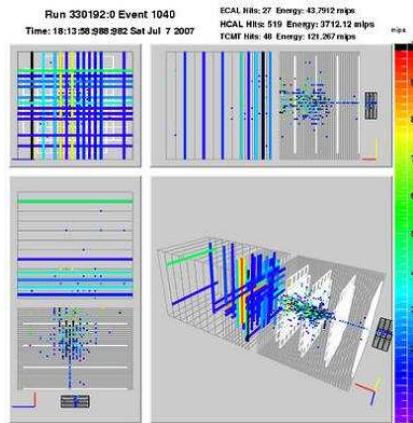


Figure 9: Run Number: 330192, Event 1040

The histograms most interesting to me are those displaying the total deposited energy in AHCAL and ECAL and the number of hits detected in the HCAL as well as in the ECAL. I also needed some information from the ADC Veto Trigger and the number of trigger events there. Furthermore I had a look on the histograms from the drift chambers and the ECAL concerning beam spread and position. It was the goal to extract numbers out of the histograms that give general information about the beam and detector stability for different experimental settings. To classify a typical event one should first have a look at the hHcalEnergy Spectrum (Figure 10). In there are already some of my fits visible that were done by my C++ program.

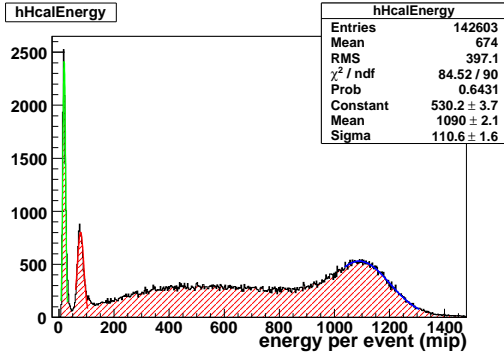


Figure 10: Fitting example of a 30 GeV pion run (Run number 500345)

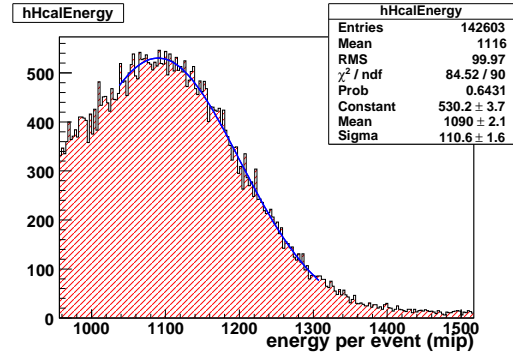


Figure 11: Graph shows the applied fit to the energy peak of a 30 GeV pion run

Beginning from the left you first can see the pedestal peak in green. The pedestal is mainly coming from random trigger events so in principal noise events internal to the data acquisition that we are collecting to make statements about the detector performance. It follows in red the muon peak. In this experiment muons are used as the so called *Minimum Ionizing Particles (MIP)*, which means a particle, that does not at all interact with matter in our calorimeter and can thus be used as a calibration tool. And finally the energy peak coming from the 30 GeV pions in this case. I wrote a C++ program that is supposed to do the needed fits to the spectrum automatically when its given a particular run number and displaying the results graphically with ROOT.

3.1 Reconstruction of the Beam Energy

As a starting point of my fit I take the calibration factor from Mip to energy in GeV. I determined it out of several energy histograms to around $Mip = 35 \text{ GeV}$. Knowing the beam energy out of the electronic logbook I was able to calculate the estimated position of the energy peak in the histogram and thus fit around this position within a range of 30 Mip to the right and 20 Mip to the left. The fit was redone twice, this time using meanvalue and sigma from the latest fit within a range of 2.5σ to the right and 0.5σ to the left. I always emphasise the right half of the peak which is more in the shape of a gaussian. The fitting result is displayed for the same 30 GeV π^- run than above in figure 11 where the initial starting point for the fit was at 1050 Mip. It became obvious that it is impossible for my program to find energy peaks of runs with a very small beam energy as I already mentioned. The energy

of these particles is so small that you almost can't see the energy peak in the histogram. That's why I exclude all runs with a beam energy smaller or equal to 4 GeV of my analysis. As a first result serve the linearity plots below (see figure 12,13). There the reconstructed energy is plotted versus the original beam energy. For low energies the fit is working fine so that the points are

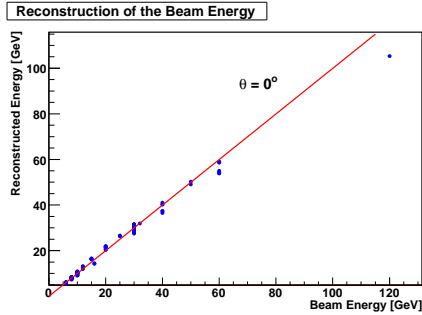


Figure 12: Linearity plot for angles of 0°

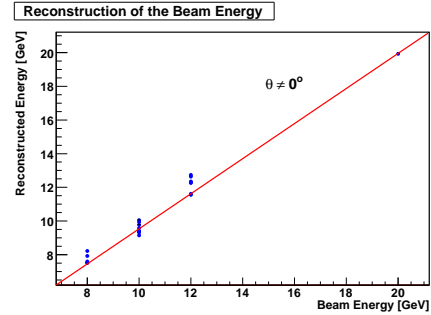


Figure 13: Linearity plot for angles unequal to 0°

matching the 1:1 line quite nice but than the resolution is getting worse. For higher energies the reconstructed energy deviates significantly from the linearity. This behaviour is already known and related to the non-linearity response of the SiPM. The run done at 120 GeV is far of the red line. As errorbars the error of the fit was taken, which is quite small and therefore not visible in the graphs. The energy reconstruction reaches a 10% precision level while points deviating from that have to be checked further (see figure 14).

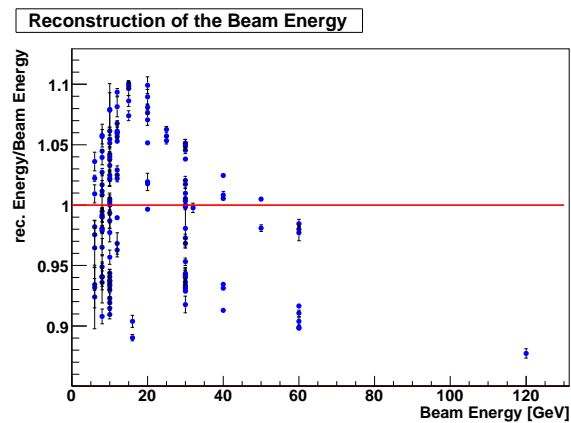


Figure 14: Linearity residual showing a precision in reconstruction of 10%

3.2 Mean Value of the Pedestal and the Muon Peak

The following step was to find the mean value of the pedestal and the muon peak. These values are gained from the hHcalEnergy histogram. Since as well as the pedestal also the muons are energy independent the position of the two peaks should not change throughout the whole experiment for different beam energies. This is therefore a nice tool to check the beam stability. But still both can move for different temperatures surrounding the experiment as it was observed during the July data taking period. An increase in temperature follows an increase in the noise level. Unfortunately those temperature corrections could not be implied to this very first online analysis study. The results for the fits around these two peaks can be seen in figure 15 for a 30 GeV run of π^- . The position of the applied cuts was fixed from 0 to 17 for the pedestal and from 17 to 31 for the muon peak. By

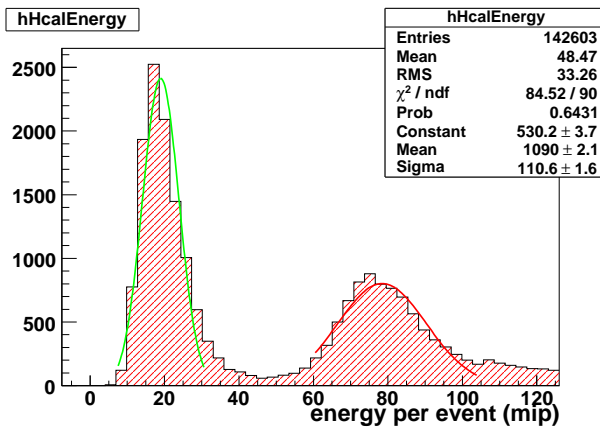


Figure 15: Fitted pedestal and muon peak for a 30 GeV pion run (run number 500345)

integrating the graph within these ranges I obtained the number of pedestal events and the number of muon events. Out of this I am able to calculate the percentage of those events over all detected events in one particular run.

3.2.1 Detector Stability - Noise Distribution

To get a feeling on how stable the detector works I plotted the mean value of the pedestal peak position versus the beam energy. As a result I received figure 16 and 17. The very right part of figure 17 shows the late July runs with no ECAL in the beamline. In figure 16 one can nicely see the two data taking periods in May and July. The shift at the right side of the graph comes from a shift in temperature from May to July. In contrast the shift at

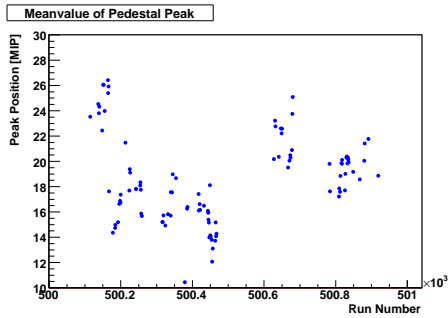


Figure 16: Mean value of the pedestal peak showing runs from May and July 2008 at Fermilab.

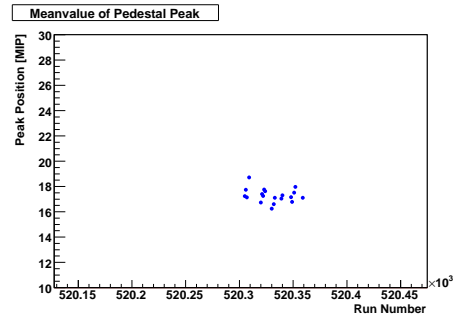


Figure 17: Mean value of the pedestal peak showing runs from the end of July 2008 (without ECAL).

the left for all the start-up and comissioning runs is not so easy explainable. I was able to show that this is certainly due to a real shift in the noise level (see figures 18, 19). It is obvious that the position of the two peaks is moving

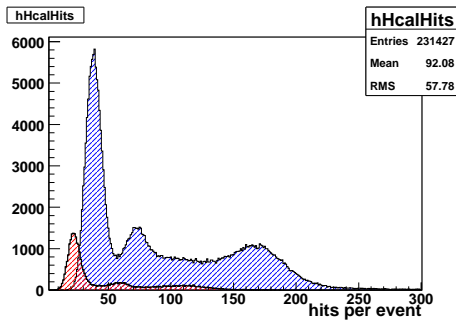


Figure 18: AHCAL Hits spectrum showing a shift in the noise level (Run number 500164 (blue), 500178 (red))

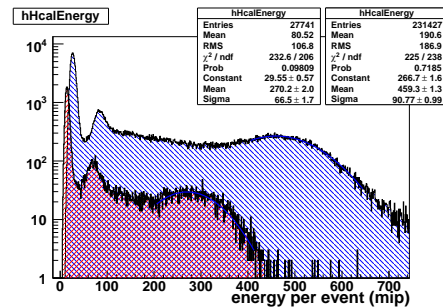


Figure 19: AHCAL Energy spectrum showing a shift in the noise level

very strongly from one run to the other. So this still needs to be checked in more detail by experts.

3.2.2 Detector Stability - Mip Calibration

Here the constance of the position of the Mip peak was tested. By having a look at figure 20 and 21 it is getting obvious that the peak moves. The expectancy value one can calculate out of the number of layers of the AHCAL (= 38) times the mean energy of a Mip (= 1.6) and times the detector

efficiency ($\approx 93-95\%$). One ends up with roughly around 60 Mip. This means that all runs with a mean peak position less than 60 Mip have to be checked again.

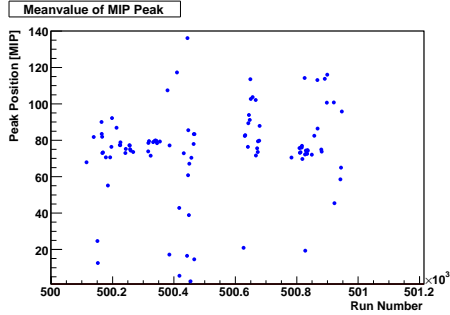


Figure 20: Mean value of the muon peak stable at around 75 Mip

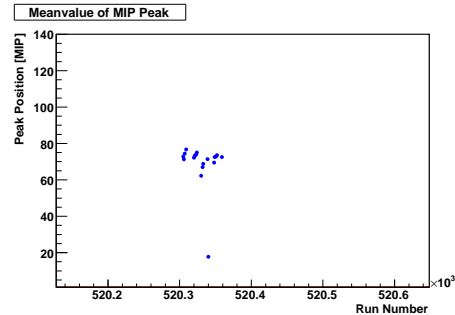


Figure 21: Mean value of the muon peak without the ECAL in the beamline

3.3 Integrated Numbers of Pedestal, Muons, Multi-Particles and Pions

By integrating the fitted peaks in the HcalEnergy spectrum within the given ranges one gets the number of pedestal and muons. Further on by looking at the Veto ADC Trigger spectrum (see figure 22) one can get the number of multi-particles in the run. Multi-particles are in most cases double particles

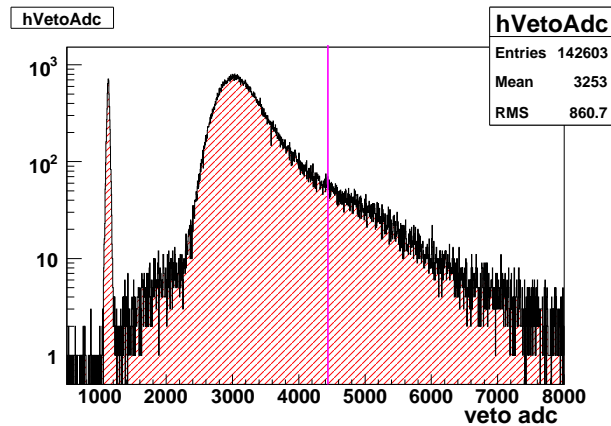


Figure 22: ADC Veto Trigger spectrum to find the number of multi-particles that are produced by showers starting already in the beampipe or by hitting

the target. So in principal they are impurities of the beam. To derive the number out of the histogram one needs to know where to start integrating. I determined the peak position of the pedestal as well as the one from the second peak. By adding the difference between these two positions to the position of the second peak one gets the position of the third peak which is equal to two particles being detected at the same time. It was decided to subtract from this number twice the rms of the second peak. So I ended up at 4440 (see purple line in the graph). Integrating from there gives you the number of double particles. The graphs 23 and 24 show the distribution of these particle numbers versus the beam energy. One can see that for

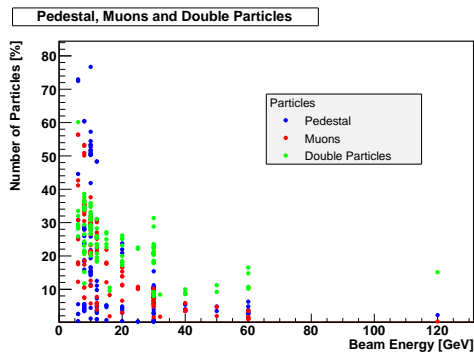


Figure 23: Number of pedestal, muons and multi-particles versus the beam energy

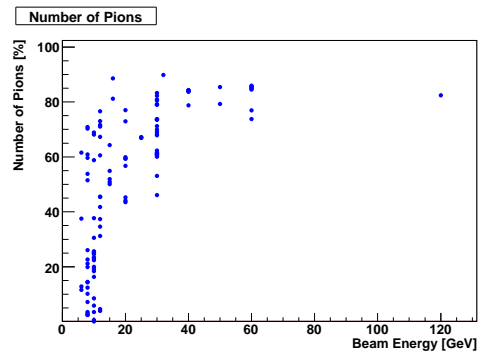


Figure 24: Number of pions versus the beam energy

low energies the contribution from the pedestal is up to 80% and decreases with higher energies. Compared to this the number of pions, which means the number of real physics events, increases also at around 80 % for high energies. So by this these two plots are somehow correlated. Surprising is the large contamination of double particles at all beam energies. So what has unfortunately happened is an overestimation of the number of double particles. This effect also is moved to figure 24 and can be observed for the points with negative percentages at low energies. Figure 25 shows how this miscalculation could have happened. The graph consist of two overlaying spectra. These two runs were chosen because the blue one was one of the runs having for the number of pions a negative percentage and the red one doesn't. There is an exponential fit applied to the two graphs. If those are extrapolated until the intersection with the x-axis they build together with the cut at 4440 a triangle. This area was handled as double particles which they in fact are not. So this number should be subtracted from the number of double particles.

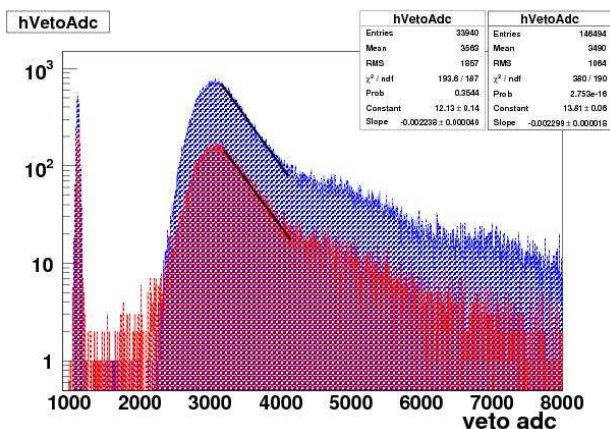


Figure 25: Overestimation of multi-particles shown by the ADC Veto Spectrum for run number 500630 (red) and 500192 (blue)

3.4 Beam Quality - Beam Position

The last chapters were covering the overall detector stability. The following ones shall describe the beam quality in more detail starting with the beam position. This for sure should be as stable as possible. To be able to make a statement about this one compares the beam position on the last drift chamber in front of the ECAL with the beam position measured on the ECAL. Therefore I fitted a gaussian at the histograms measured by the drift chamber 1 (see figure 26, 27). The fit is done in a way that it ignores the right part of the histogram. This is where the beam hits the edge of the drift chamber and therefore is creating an inefficient region. To determine the position of the beam on the ECAL the histogram hEcalYX was projected on the x- and y-axis and the mean value for both defined (see figure 28, 29). For all the four plots run 500345 was used. As resulting plots one obtains figures 30 and 31.

The beam should be centered on the drift chamber which corresponds to zero in the graph. However it is shifted slightly to something around 1. Another point that has to be checked in the near future. The relative offset to the ECAL is due to the experimental setup. One sees that the two graphs are consistent with each other. Both showing that for lower energies the beam position is getting less centered. Since the drift chamber is 8x8 cm large it is suggested to have a closer look on all runs with a beam position farer away than 4 cm from the center of the drift chamber. In graph 31 the points lying on the x-axis are runs where the ECAL was removed out of the beamline that's why there are no entries in the ECAL histogram.

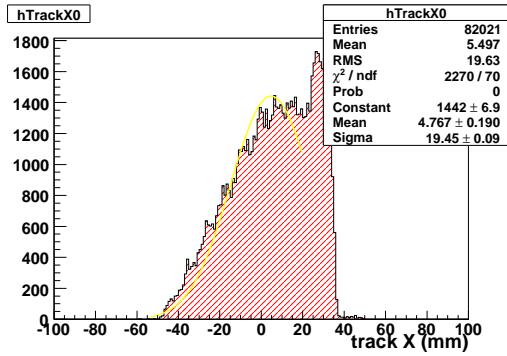


Figure 26: Beam position at the drift chamber DC1 in x-direction

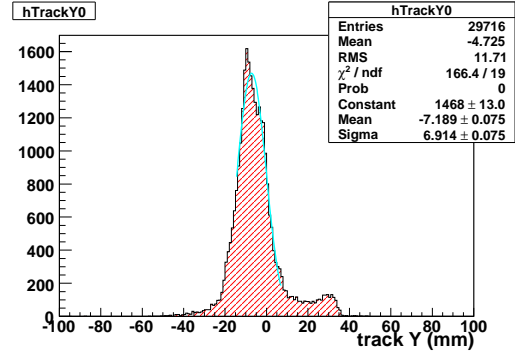


Figure 27: Beam position at the drift chamber DC1 in y-direction

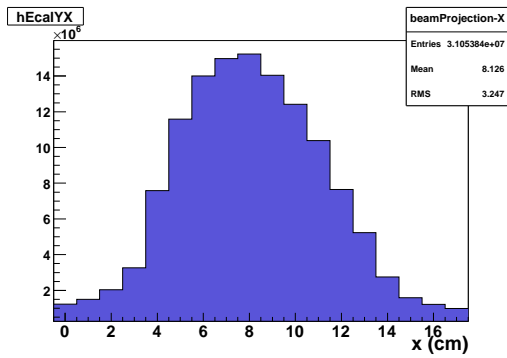


Figure 28: Beam position at the ECAL in x-direction

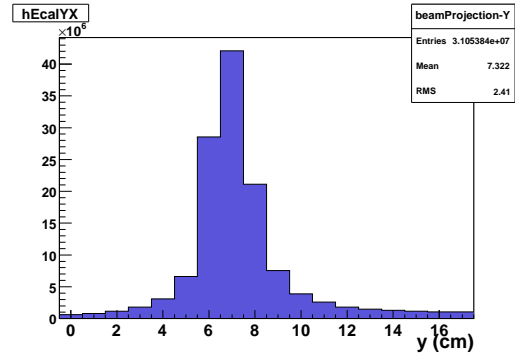


Figure 29: Beam position at the ECAL in y-direction

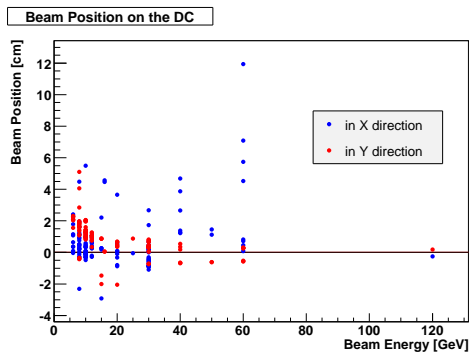


Figure 30: Beam position at the drift chamber DC1

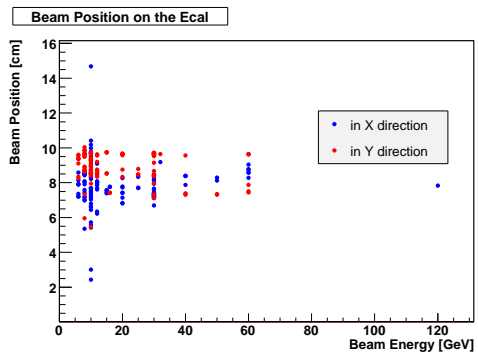


Figure 31: Beam position at the ECAL

3.5 Beam Quality - Beam Spread

To obtain the beam spread I used the same graphs this time determining the rms instead of the mean value for all four plots. The two dimensional histogram hEcalYX (figure 32) already used before gives already an idea on how the results should look like. Figures 33 and 34 are the resulting plots.

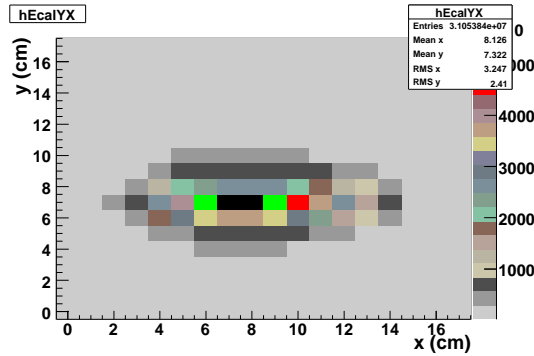


Figure 32: Two dimensional histogram hEcalYX monitoring the beam spread at the ECAL for run number 500345.

As you can see the beam spread is increasing towards lower energies where the beam can't be focused as good as for higher energies. Also the beam is always broader in x- than in y-direction for all energies. Here all runs with a beam broader than 3 cm in one direction should be checked again.

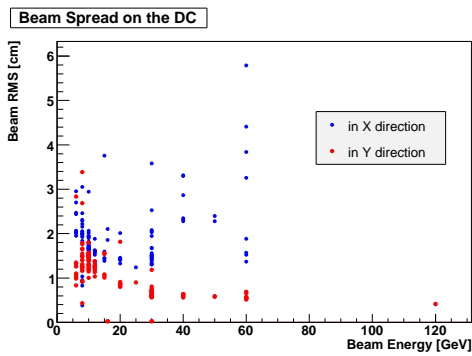


Figure 33: Beam spread at the drift chamber DC1

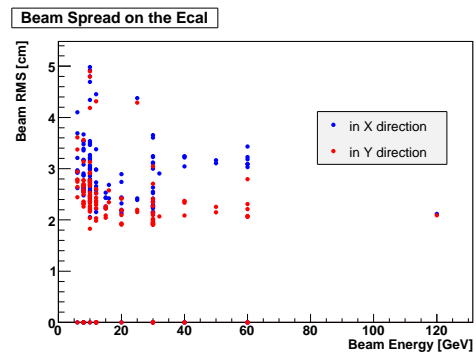


Figure 34: Beam spread at the ECAL

4 Conclusions and Outlook

The highly granular analogue hadronic calorimeter has been successfully operated at FNAL in 2008. Furthermore a first analysis was performed with the Online Monitoring Histograms by myself during the last 8 weeks. A list with runs that have to be checked and those that can easily be used for further analysis is created. But energies smaller or equal to 4 GeV still have to be checked as well as measured points deviating a lot from the expectations. To be able to do so the next step will be to use Root-Ntuples to analyse the data in more detail.

5 References

- [1] Marius Groll, *Construction and Commissioning of a Hadronic Test-Beam Calorimeter to Validate the Particle-Flow Concept at the ILC*
- [2] Benjamin Lutz, *Commissioning of the Readout Electronics for the Prototypes of a Hadronic Calorimeter and a Tailcatcher and Muon Tracker*
- [3] Nanda Wattimena, *Commissioning of an LED Calibration & Monitoring System for the Prototype of a Hadronic Calorimeter*
- [4] Homepage of the FLC subgroup for the AHCAL, www-flc.desy.de/hcal
- [5] Homepage of the CALICE testbeam program at FNAL-MTBF, www.hep.phy.cam.ac.uk/~gmavroma/calice/testbeam/testbeam.html